LETTER

Generation of nonlinear Airy beams with switchable acceleration direction

IOP Publishing
Letters
Journal of Optics
J. Opt. **25** (2023) 07LT01 (5pp)
https://doi.org/10.1088/2040-8986/acd392

Letter

Generation of nonlinear Airy beams with switchable acceleration direction

Dong Wu[1], Zihang Zhang[1], Chaowei Wang[1,*], Leran Zhang[1], Liqun Xu[1], Dunzhao Wei[2], Wei Xiong[3], Jiawen Li[1], Yanlei Hu[1], Jiaru Chu[1] and Yang Chen[1,*]

[1] CAS Key Laboratory of Mechanical Behavior and Design of Materials, Department of Precision Machinery and Precision Instrumentation, University of Science and Technology of China, Hefei, Anhui 230027, People's Republic of China
[2] State Key Laboratory of Optoelectronic Materials and Technologies, School of Physics, Sun Yat-Sen University, Guangzhou 510275, People's Republic of China
[3] Wuhan National Laboratory for Optoelectronics and School of Optical and Electronic Information, Huazhong University of Science and Technology, Wuhan 430074, People's Republic of China

E-mail: chaoweiw@ustc.edu.cn and cyang_phys@ustc.edu.cn

Received 10 March 2023, revised 4 May 2023
Accepted for publication 8 May 2023
Published 31 May 2023

Abstract

Airy beams, which propagate along a curved trajectory, have been widely utilized in optical tweezers, biomedical analysis, and material processing. However, the dynamic regulation of nonlinear Airy beams is still challenging. Here, we demonstrate directionally switchable nonlinear Airy beams via three-dimensional (3D) nonlinear photonic crystals (NPCs) fabricated by the femtosecond laser erasing technique. The 3D NPCs contain several sequential arrays of spatially modulated nonlinearities with different spatial frequencies and cubic coefficients. By tuning the wavelength of the fundamental beam, the quasi-phase-matching condition can be switched to modulate the acceleration direction and wavelength of the generated nonlinear Airy beam. This offers a versatile platform for dynamic nonlinear Airy beam generation, paving the way for applications in optical trapping, optical communication, and biomedical imaging.

Keywords: nonlinear photonic crystals, Airy beams, femtosecond laser erasing, quasi-phase-matching

(Some figures may appear in colour only in the online journal)

1. Introduction

It is commonly known that light propagates along a straight line. However, if light can travel along curved trajectories, new phenomena and applications are enabled such as optical illusions and cloaking [1–4]. An Airy beam is a typical light beam that propagates along a parabolic trajectory in free space. Its spatial evolution can be described by the Schrodinger equation [5]. Since the first observation of Airy beams in 2007 [6], their unique properties of self-bending [7, 8], self-healing [9, 10], and non-diffraction [6] have drawn considerable attention from both academia and industry. These properties promise a plethora of applications, such as filamentation [11], biomedical imaging [12], plasmons [13], and material processing [14], especially through the use of optical trapping to control particles [15–19]. To date, Airy beams have been mostly investigated in the regime of linear optics (e.g., spatial light modulator [20], cylindrical lens [21, 22] and liquid crystals [23]), but the incorporation of nonlinear optical processes into

* Authors to whom any correspondence should be addressed.

Airy beams will introduce new wavelengths as an extra degree of freedom to further expand the functionalities of Airy-beam-based devices [24, 25].

In the study of nonlinear Airy beams, one of the most challenging and important issues is the active modulation and multiplexing of the propagation properties of nonlinear Airy beams, such as the acceleration direction and caustic trajectory. Although metasurfaces can be utilized for tuning the propagation trajectory of Airy beams [26], they cannot be applied to the nonlinear Airy beams due to their low nonlinear conversion efficiency. 1D or 2D nonlinear photonic crystals (NPCs) provide an alternative platform for dynamically controlling nonlinear Airy beams [27–29]. However, most have stringent requirements and suffer from low flexibility and limited working frequencies. Therefore, there is an urgent need to realize efficient generation and flexible manipulation of nonlinear Airy beams. Femtosecond laser writing is one of the suitable techniques for solving this issue since it can efficiently create three-dimensional (3D) structures in different materials [30, 31].

Here, we demonstrate the dynamic modulation of the acceleration direction of nonlinear Airy beams based on 3D NPCs fabricated by femtosecond laser erasing technique. 3D NPCs [32, 33] are designed to provide a reciprocal vector for compensating the phase mismatch in the longitudinal direction, such that nonlinear Airy beams are generated with a high conversion efficiency of up to 1.3×10^{-5}. Furthermore, a unique recipe is developed for actively controlling the acceleration direction of the generated nonlinear Airy beams, where sequential nonlinear photonic structures with different spatial carrier frequencies and cubic coefficients are fabricated inside an individual nonlinear crystal. In this way, the acceleration direction of nonlinear Airy beam can be adjusted by changing the wavelength of the fundamental beam. We believe this method promises more flexible manipulation of nonlinear Airy beams for applications in optical tweezers, biomedical analysis, and material processing.

2. Design of 3D NPCs for generation of nonlinear Airy beams

3D nonlinear structures are composed of periodic 2D nonlinear structures, so we first obtain the distribution of the 2D nonlinear structure in order to determine the whole structure [34]. In this process, we use a variation of a binary computer-generated hologram (CGH) to calculate the $\chi^{(2)}$ susceptibility pattern, which can generate the desired beam shape in the second harmonic (SH) directly [35, 36]. However, the femtosecond laser direct writing technique can only realize binary amplitude modulation in NPCs, so we use the function T expressed as

$$T(s) = \begin{cases} 1, & s \geqslant 0 \\ 0, & s < 0 \end{cases}. \tag{1}$$

The first CGH sub-arrays are incorporated into a single $LiNbO_3$ crystal along the propagation direction, i.e.m the y-axis. The CGH of the 2D NPCs can be expressed as

$$f(x,z) = T\left\{\cos\left[G_x x - \arg\left(E_{2\omega}\right)\right] - \cos\left[\sin^{-1}\mathrm{amp}\left(E_{2\omega}\right)\right]\right\}, \tag{2}$$

where $E_{2\omega}$ is the designed SH field, with its amplitude and phase denoted by the '*amp*' and '*arg*' functions, respectively. G_x is a reciprocal vector in the x–z plane, also known as the carrier frequency, and affects the diffracted angle of $E_{2\omega}$. We need the other reciprocal vector G_y to meet the quasi-phase-matching (QPM) condition, which is provided by the periodic modulation structure along the y-axis. Therefore, the CGH sub-arrays of the 3D NPCs can be expressed as

$$\begin{aligned} f(x,y,z) = T\{&\cos\left[G_x x - \arg\left(E_{2\omega}\right)\right] \\ &- \cos\left[\sin^{-1}\mathrm{amp}\left(E_{2\omega}\right)\right]\} \times T\left[\cos\left(G_y^i y\right)\right], \end{aligned} \tag{3}$$

where $T\left[\cos\left(G_y^i y\right)\right]$ is the modulation function along the y-axis. The Fourier transform of equation (1) is given by

$$\begin{aligned} f(x,y,z) = &\sum_{m,n} c_{m,n} \sin\left[m \times \sin^{-1}\mathrm{amp}\left(E_{2\omega}\right)\right] \\ &\times e^{i(mG_x x + nG_y y)} e^{-i\mathrm{marg}(E_{2\omega})}, \end{aligned} \tag{4}$$

where m and n are the orders of the reciprocal vectors along G_x and G_y, respectively, and $c_{m,n}$ is the corresponding Fourier coefficient.

The higher the order of reciprocal vector is, the weaker the strength of the SH becomes. Clearly, we only consider the $\pm$1st order. As $m = n = 1$, equation (4) reduces to

$$f(x,y,z) = c_{1,1} E_{2\omega} e^{i(G_x x + G_y y)}, \tag{5}$$

which recovers the designed SH fields.

When using the Airy beam as the target, note that the Fourier transform of Airy beams is in the form of a Gaussian beam superimposed cubic phase factor. To separate the other diffraction orders from the zero-order beam, we superimpose the sparkly grating with it, so the $\chi^{(2)}$ of 3D NPCs can be written as

$$\begin{aligned} \chi^{(2)}(x,\mathrm{y},z) &= d_{33} - d_{33}(1-v) \times f(x,y,z) \\ &= d_{33} - d_{33}(1-v)\, c_{1,1} e^{i(G_x x + G_y y)} e^{if_c x^3 + if_z z} \end{aligned} \tag{6}$$

where d_{33} is the involved nonlinear coefficient, v is defined as the modulation depth, and f_z and f_c are the carrier frequency and strength of the cubic modulation in the transverse direction, respectively. It is clear that the hologram consists of the cubic gradient phase along the x-axis and linear gradient phase along the z-axis from equation (6). Figure 1(a) shows the generation of the cubic phase diagram of Airy beams, and we obtain the 3D nonlinear structure by arranging the binary hologram according to the design period.

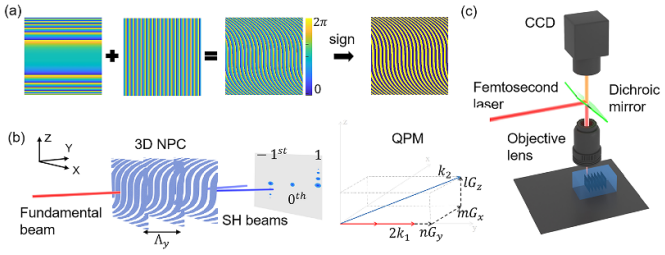

Figure 1. (a) The design process of a linearly gradient phase integrated cubic hologram. (b) Schematic representation of the spatial modulation of nonlinearity in 3D NPCs and the QPM configurations for reconstructing multiple SH beams. Here, the ±1st orders show enhanced SH patterns. (c) System for processing 3D NPCs.

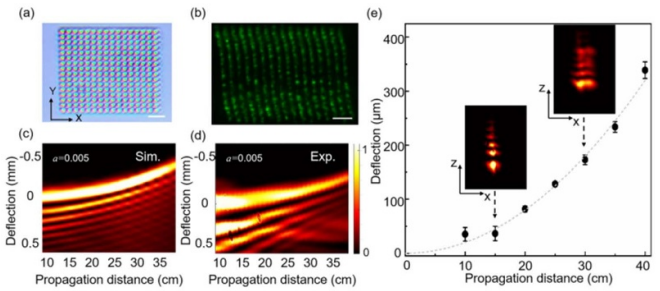

Figure 2. Generation of nonlinear Airy beam. (a) Top view of the arrays via optical microscope (length of scale bar, 10 μm). (b) Confocal SH image of the cross-section in the x–z plane (length of scale bar, 10 μm). (c) Theoretical simulation and (d) experimental results of SH Airy beam in the case of $a = 0.005$ ($f = 150$ mm). a is the cubic term coefficient of the grating structure. (e) Dependence of the longitudinal deflection of nonlinear Airy beam along the y-axis. Black dots with error bars are experimental results, and the gray dashed line is the simulated curve. Images captured at 15 and 30 cm are inserted above the corresponding dots.

Figure 1(b) shows the switchable reconstruction process through the QPM condition, which can be expressed as

$$\boldsymbol{k}_{2\omega} - 2\boldsymbol{k}_{\omega} - \boldsymbol{G}_x - \boldsymbol{G}_y = 0 \tag{7}$$

where $\boldsymbol{k}_{\omega}$ and $\boldsymbol{k}_{2\omega}$ are wavevectors of the fundamental beam and the diffracted SH beam, respectively. Since the Airy beam only requires 1D optical manipulation, the parameter l is not mentioned. When the full QPM condition of equation (7) is satisfied, the conversion efficiency of the ±1st order will be maximized.

3. Experimental generation of nonlinear Airy beams

In the experiment, the femtosecond laser erasing technique was used to fabricate the cubic-phase-grating array in a y-cut $LiNbO_3$ crystal, as shown in figure 1(c). The femtosecond laser beam (Legend Elite-1K-HE, Coherent, USA, 1 kHz repetition rate, 800 nm center wavelength, and 104 fs pulse width) was focused into the crystal using a 50× objective lens with a numerical aperture of 0.8, and the laser power was set to 110 μW. Optical and SH microscopy images of the 3D nonlinear photonic structure are shown in figures 2(a) and (b); it has dimensions of 50 μm (x) × 33 μm (z) in the x–z plane and 16 periods along y-axis with an interval of 2.75 μm.

The schematic of the experimental setup is then exhibited as follows. The fundamental wave (FW) output was from a Ti: sapphire oscillator (Spectra-Physics Mai Tai HP) with a center wavelength of 800 nm, pulse width of 75 fs, and repetition rate of 80 MHz. The FW was focused on the position of the structures by a lens ($f = 150$ mm), and an objective lens was placed behind the crystal to perform an optical spatial Fourier transform to the SH beam. The output far-field SH patterns were recorded by a charge-coupled device camera. The rest of the FW was blocked by a short pass filter. The images from the camera are shown in the insert of figure 2(e), in which we reduced the camera gain to avoid overexposure.

It is further necessary to analyze the propagation dynamics to exhibit the typical self-acceleration feature of Airy beams. The output far-field SH patterns were recorded along the propagation direction with an interval of 1 mm and total distance of 10 cm from the Fourier plane of the objective lens, and multiple sections were combined into a single top view, as shown in figure 2(d), showing good consistency with the simulation (figure 2(c)). To characterize the propagation curve conveniently and accurately, we measured the deflection in the y-direction of the main lobe center, as shown in figure 2(e). The experimental curved trajectory of the nonlinear Airy beam exhibits a parabolic curve and the deflection exceeds 300 μm, matching well with the simulation data. In the process of simulation, we created a cubic phase hologram according to equation (6). Next, a Gaussian beam is passed through the hologram and diffracted to produce a pair of 1D Airy beams. We intercepted a column of pixels on the diffraction plane every 0.1 mm from the Fourier plane and synthesized the trajectory, as shown in figures 4(b) and (d).

Figure 3(a) presents the far-field SH patterns and output power dependence on the wavelengths of the fundamental beam. When the fundamental beam wavelength is set to 798 nm, the far-field SH pattern is the clearest and the output power is the highest, which is basically consistent with the theoretical QPM wavelength of 800 nm. The deviation between the measured and calculated values stems from the imperfection of the laser erasing process. When the FW tunes away from the theoretical matching wavelength, the SH power drops rapidly and the far-field SH patterns dim out. Figure 3(b) presents the dependence of the output power of the SH beam on the fundamental beam power at the wavelength of 800 nm. At an input power of 1.5 W, the peak conversion efficiency reaches 1.3×10^{-5}, for the first diffraction order.

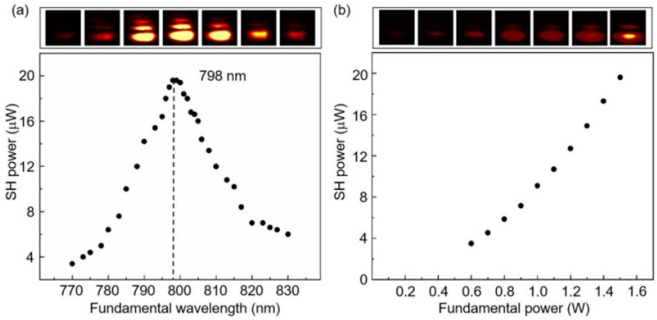

Figure 3. (a) Dependence of output power of the first diffraction order on the fundamental wavelength at a pump power of 1.5 W. (b) Dependence of output power of the SH Airy beam on pump power at the wavelength of 800 nm.

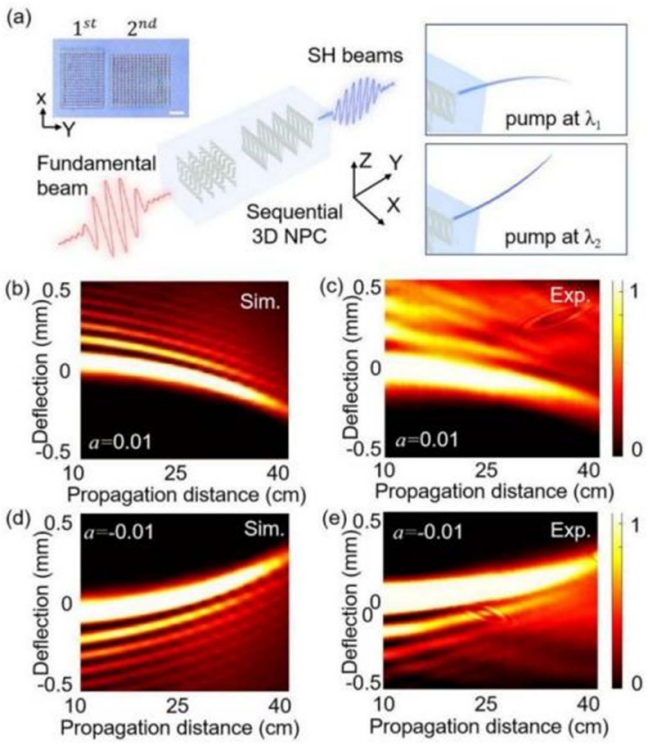

Figure 4. (a) Model of 3D NPC with sequential structures. Top view (length of scale bar, 15 μm) (b), (d) theoretical simulations and (c), (e) experimental results of SH Airy beams, generated by the first (top) or second (bottom) structure, respectively, in the case of $a = 0.01$ ($f = 60$ mm).

4. Generation of nonlinear Airy beam with switchable curved directions

To realize Airy light generation with switchable acceleration direction, we design and fabricate a 3D NPC containing a pair of cubic-phase-grating arrays. Optical microscopy images of the two-sequential 3D nonlinear photonic structures are shown in the insert of figure 4(a). They have dimensions of 50 μm (x) $\times$ 33 μm (z), and 56 μm (x) $\times$ 33 μm (z) in the x–z plane respectively, and 16 periods along y-axis with intervals of 2.5 and 3.5 μm respectively. The two sub-arrays have different spatial frequencies and periods, so different wavelengths can be selected to interfere with the corresponding structure, thereby realizing the selective output of the far-field diffracted SH field. The SH patterns of the simulation and experiment are both shown in figures 4(b)–(e). When the wavelength of the fundamental beam is 780 nm, the second array works and meets the QPM conditions well. The acceleration direction of the generated nonlinear Airy light is toward the downward side, as shown in figure 4(c). Switching the wavelength to 850 nm, the fundamental beam interferes with the first array, and the acceleration direction of the generated nonlinear Airy light is toward the upward side (figure 4(e)). These results are supported by the numerical simulations in figures 4(b) and (d). Therefore, by designing a sequential 3D nonlinear photonic structure with suitable carrier frequencies and periods, we can switch directions of the output Airy beam by tuning the wavelength of the fundamental beam. Furthermore, by changing the cubic-phase-grating array with different coefficients f_c, a switchable self-acceleration angle of the nonlinear Airy beam can also be achieved by these sequential 3D nonlinear photonic structures.

5. Conclusion

We fabricate sequential 3D nonlinear photonic structures in $LiNbO_3$ based on femtosecond laser-erasing technique, and present the generation of nonlinear Airy beams with switchable curved directions. Benefiting from the high flexibility of structure design and fabrication, multiple wavelength-controlled nonlinear Airy beams have been realized. The nonlinear conversion efficiency and available curved trajectories could be further improved if the number of periods in the propagation direction is increased. This provides a paradigm shift for efficiently producing and actively controlling nonlinear Airy beams, which have great applications in optical trapping, optical communication, and biomedical imaging.

Data availability statement

All data that support the findings of this study are included within the article (and any supplementary files).

Acknowledgments

This work was supported by the National Key Research and Development Program of China (No. 2021YFF0502700), CAS Project for Young Scientists in Basic Research (No.

YSBR-049), the National Natural Science Foundation of China (Nos. 61927814, 52122511, 62005262, 52075516), the China Postdoctoral Science Foundation (2021T140649), Major Scientific and Technological Projects in Anhui Province (202103a05020005, 202203a05020014), the USTC Research Funds of the Double First-Class Initiative (YD2340002009), the Open Project of Wuhan National Laboratory for Optoelectronics (No. 2019WNLOKF014), and Guangdong Natural Science Funds for Distinguished Young Scholars (2022B1515020067). We acknowledge the Experimental Center of Engineering and Material Sciences at USTC for the fabrication and measuring of samples. This work was partly carried out at the USTC Center for Micro and Nanoscale Research and Fabrication.

ORCID iD

Yang Chen https://orcid.org/0000-0002-8501-5417

References

[1] Li J and Pendry J B 2008 *Phys. Rev. Lett.* **101** 203901
[2] Valentine J, Li J, Zentgraf T, Bartal G and Zhang X 2009 *Nat. Mater.* **8** 568–71
[3] Gabrielli L H, Cardenas J, Poitras C B and Lipson M 2009 *Nat. Photon.* **3** 461–3
[4] Cai W, Chettiar U K, Kildishev A V and Shalaev V M 2007 *Nat. Photon.* **1** 224–7
[5] Berry M V and Balazs N L 1979 *Am. J. Phys.* **47** 264–7
[6] Siviloglou G A, Broky J, Dogariu A and Christodoulides D N 2007 *Phys. Rev. Lett.* **99** 213901
[7] Siviloglou G A, Broky J, Dogariu A and Christodoulides D N 2008 *Opt. Lett.* **33** 207–9
[8] Siviloglou G A and Christodoulides D N 2007 *Opt. Lett.* **32** 979–81
[9] Baumgartl J, Mazilu M and Dholakia K 2008 *Nat. Photon.* **2** 675–8
[10] Broky J, Siviloglou G A, Dogariu A and Christodoulides D N 2008 *Opt. Express* **16** 12880–91
[11] Polynkin P, Kolesik M, Moloney J V and Siviloglou G A 2009 *Science* **324** 229–32
[12] Jia S, Vaughan J C and Zhuang X 2014 *Nat. Photon.* **8** 302–6
[13] Salandrino A and Christodoulides D N 2010 *Opt. Lett.* **35** 2082–4
[14] Mathis A, Courvoisier F, Froehly L, Furfaro L, Jacquot M, Lacourt P A and Dudley J M 2012 *Appl. Phys. Lett.* **101** 071110
[15] Lu W L, Chen H J, Liu S Y and Lin Z F 2017 *Opt. Express* **25** 23238–53
[16] Lu W L, Sun X, Chen H J, Liu S Y and Lin Z F 2018 *J. Opt.* **20** 125402
[17] Lu W L, Chen H J, Guo S D, Liu S Y and Lin Z F 2018 *Opt. Lett.* **43** 2086–9
[18] Lu W L, Chen H J, Liu S Y and Lin Z F 2019 *Phys. Rev.* A **99** 013817
[19] Lu W L, Chen H J, Liu S Y and Lin Z F 2022 *Phys. Rev.* A **105** 043516
[20] Hu Y, Zhang P, Lou C B, Huang S, Xu J J and Chen Z G 2010 *Opt. Lett.* **35** 2260–2
[21] Yalizay B, Soylu B and Akturk S 2010 *J. Opt. Soc. Am.* A **27** 2344–6
[22] Papazoglou D G, Suntsov S, Abdollahpour D and Tzortzakis S 2010 *Phys. Rev.* A **81** 061807
[23] Dai H T, Sun X W, Luo D and Liu Y J 2009 *Opt. Express* **17** 19365–70
[24] Liu Y *et al* 2021 *Adv. Opt. Mater.* **9** 2001776
[25] Liu H, Zhao X, Li H, Zheng Y and Chen X 2018 *Opt. Lett.* **43** 3236–9
[26] Fan Q *et al* 2019 *Nano Lett.* **19** 1158–65
[27] Ellenbogen T, Voloch-Bloch N, Ganany-Padowicz A and Arie A 2009 *Nat. Photon.* **3** 395–8
[28] Trajtenberg-Mills S, Juwiler I and Arie A 2017 *Optica* **4** 153–6
[29] Dolev I, Ellenbogen T and Arie A 2010 *Opt. Lett.* **35** 1581–3
[30] Yang L, Mayer F, Bunz U H F, Blasco E and Wegener M 2021 *Light Adv. Manuf.* **2** 296–312
[31] Yu H, Ding H, Zhang Q, Gu Z and Gu M 2021 *Light Adv. Manuf.* **2** 31–38
[32] Wei D *et al* 2018 *Nat. Photon.* **12** 596–600
[33] Wei D *et al* 2019 *Nat. Commun.* **10** 4193
[34] Chen P *et al* 2021 *Light Sci. Appl.* **10** 146
[35] Lee W 1979 *Appl. Opt.* **18** 3661–9
[36] Trajtenberg-Mills S, Juwiler I and Arie A 2015 *Laser Photonics Rev.* **9** L40–L44